IJBPAS, August, 2020, 9(8): 1798-1811

ISSN: 2277–4998

International Journal of Biology, Pharmacy and Allied Sciences (IJBPAS)

'A Bridge Between Laboratory and Reader'

www.ijbpas.com

ENHANCED PHOTOCATALYTIC DEGRADATION EFFICIENCY OF GREEN OXIDANT COMBINED STRONTIUM AND NITROGEN-CODOPED TiO_2 OVER REACTIVE ORANGE 30 UNDER NATURAL SUN LIGHT IRRADIATION

SIVAKUMAR M[1, 2], RAVISHANKAR M[*2] KRISHNAN E[2&3] AND SIVAKUMAR S[1]

[1]Department of Chemistry, E. R. K Arts and Science College, Dharmapuri, Tamilnadu, INDIA

[2]Department of Chemistry, Rajah Serfoji Government College (Autonomous), Thanjur, Tamilnadu, INDIA

[3]Department of Chemistry, PSA college of Arts and Science, Dharmapuri, Tamilnadu, INDIA

***Corresponding Author: E Mail: ravishankar1in@yahoo.co.in**

Received 6th Dec. 2019; Revised 4th Jan. 2020; Accepted 4th Feb. 2020; Available online 1st Aug. 2020

https://doi.org/10.31032/IJBPAS/2020/9.8.5121

ABSTRACT

The photocatalytic activity of Sr, N-codoped TiO_2 photocatalysts was investigated by the degradation of Reactive Black 5 (RB 5) under natural sunlight irradiation. A series of Sr, N-codoped TiO_2 photocatalysts with different dopant concentrations (0.001 M%, 0.003 M %, 0.005 M %, 0.007 M %, and 0.009 M %) were synthesized by sol-gel route. Initially, photocatalytic activity of the pure TiO_2 was hindered due to its poor surface properties and low utilization of visible light. To minimize these bottle neck drawbacks of TiO_2 photocatalyst, the doping treatment of Strontium and Nitrogen. The photocatalytic activity of Sr, N-codoped TiO_2 photocatalysts was remarkably higher than that of the as-prepared sample. The highlighted photocatalytic properties of Sr, N-codoped TiO_2 were confirmed by X-ray powder diffraction (XRD), Scanning electron microscopy (SEM), UV-visible diffused reflectance spectroscopy (UV-DRS) and Photoluminescence spectra (PL). 0.007% Sr, N-codoped TiO_2 has photostability and long durability. Further, green oxidant (H_2O_2) combined photocatalytic activity process carried out with highly reactive 0.007% Sr, N-codoped TiO_2 photocatalyst.

Keywords: Sr, N-Codoped TiO_2, sol-gel route, Photocatalytic Degradation, Reactive Orange 30 and Natural Sun Light, green oxidant, semiconductor

1. INTRODUCTION

Nowadays, the presence of harmful organic pollutant in wastewater effluents causes serious environmental problems and therefore purification of contaminated water is one of the most interesting challenges. It will be easy to decompose toxic materials in air or wastewater using sun light and visible light. Certainly using solar light is an optimal way to treat wastewater problem due to its continuous energy and free of charge **[1]**. Semiconductor photocatalysts that can convert solar energy into chemical energy offer a viable approach to the solution of environmental problems. Among the various oxide and non-oxide semiconductor photocatalysts, TiO_2 appears to be the most promising photocatalyst because of its excellent oxidative ability and chemical stability. Anatase TiO_2 has been investigated as a promising photocatalytic semiconductor for decades due to its high photocatalytic activity, resistance to photocorrosion, photostability, low cost, and nontoxicity **[2−5]**. Unfortunately, the photocatalytic activity of anatase phase TiO_2 semiconductor is constrained to the UV region due to its large band gap (Eg = 3.2 eV), which carries approximately 4% of the solar radiation at the Earth's surface. Another drawback that hindered the actual application of anatase is its fast recombination rate of photogenerated electron−hole pairs, that is, the low quantum efficiency. In recent years, the main strategy toward achieving activity under visible light is nonmetal doping, such as B, C, N, F, and S **[6−14]**. The success in nitrogen doping and increasing the photocatalytic activity of TiO_2 semiconductor in visible light region provides good opportunities for extensive applications to remove organic pollutants. Unfortunately, in many cases, the UV photocatalytic activities are relatively low. Therefore, it is a challenging issue to develop a photocatalyst with higher photocatalytic activity under both ultraviolet and visible light irradiation **[15, 16]**. In addition, codoping with different types of ions has also been proposed by many researchers to reach some synergetic effects between codoped ions. For instance, Huang *et al*. **[17]** and Ding *et al*. **[18]** reported that the photocatalytic activity of TiO_2 could be further enhanced by metal and nonmetal codoping demonstrated that the visible absorption of TiO_2 was able to be greatly improved photocatalytic activity.

Hence, the selectivity of electron acceptors becomes very important. The addition of irreversible electron acceptors, such as potassium bromate ($KBrO_3$),

hydrogen peroxide (H_2O_2) and ammonium peroxydisulphate $(NH_4)_2S_2O8$ to the oxygen molecule supported dye solution, it can be produce the powerful oxidizing species such as BrO_3^-, •OH and SO_4^-. These oxidizing species utilized the more photogenerated electrons than the O_2^{2-} species due to it has a higher reduction potential. So that, it also contribute to minimize the recombination of the electron-hole pair's charges **[19]**. Therefore, we have studied the effect of electron acceptors such as hydrogen peroxide and ammonium peroxydisulphate on the photocatalytic degradation of the RB 4.

In this study, Sr-N co-doped TiO_2 nanoparticles were prepared by a simple sol-gel method, and their intrinsic characteristics were analyzed using X-ray diffraction (XRD), scanning electron microscopy (SEM), UV-vis spectroscopy and photoluminescence study. The photocatalytic degradation performance of as-synthesized TiO_2 samples were evaluated by the degradation rate of reactive black 5 (RB 5) under solar light irradiation, and the synergistic effect of Sr and N co-doping was discussed. By making use of the codoping of nitrogen and strontium in TiO_2, we expect that the resultant TiO_2 nanomaterials will have high visible-light photocatalytic activity and can be used in practice.

2. MATERIALS AND METHODS

This chapter deals with the method of preparation of catalyst, characterization techniques, Instrumental techniques and the experimental set-up used for the carrying out the photocatalytic study.

2.1 Chemical Used

Titanium tetrachloride (99.5%), Stranstium chloride and Urea supplied by Loba Chemie Pvt. Ltd, borox (AR) 99% and Ammonia solutions (33%) by Qualigens were used for the preparation of the Sr, N codoped TiO_2 photo catalyst. Reactive black 5 (industrial grade) supplied by Vexent Dyeaux India Pvt. Ltd, Mumbai (minimum dye content 80%) was used for the preparation on model effluent for photocatalytic studies. Hydrochloric acid (35%), were used for photocatalytic performence. Dye solutions for photocatalytic studies were prepared in double distilled water. **Analysis:** Hydrogen peroxide used as green oxidant for combined oxidant photocatalytic degradation.

2.2 Preparation of Sr, N-codoped TiO_2 Photocatalyst

TiO_2 and Sr, N-codoped TiO_2 used for the photocatalytic studies were synthesized in sol-gel method as reported b. In the typical synthesis 5 ml of Titanium tetrachloride was added into 250ml of ice cold distilled water with vigorous stirring for

several minutes. The hydrolysis of $TiCl_4$ in the dilute aqueous solution could be expressed as:

$$TiCl_4 + H_2O \longrightarrow TiO_2 + 4H^+ + 4\,Cl^-$$

The hydrolysis reaction gives colloid solution with several nano-sized TiO_2 particles. By adding ammonia to the colloid solution, the OH^- neutralizes H^+ to make the flocculation of TiO_2. The precipitate was then washed with distilled water and was centrifugally separated by several times and was followed by drying at 100°C to remove part of the absorbed water. In N, F-Codoping TiO_2 process, the above TiO_2 and N, Sr precursors were mixed with various molar ratios (N, Sr/Ti=0 to 0.25%) and then the homogeneously mixed. Gel was dried at 100°C to remove part of the absorbed water. The solid obtained after drying was grounded in an agate mortar and mixture was pressed into a ceramic crucible and then calcinate at different temperatures 450°C for 4hr solid phase reaction. The synthesis process is shown in flow chart.

2.3 Characterization

The powder X-ray diffraction patterns of the photocatalysts were recorded using Bruker AXS D8 Advance X-ray diffractometer with Cu-K□ radiation (□□= 0.15406 nm) in the 2□□range 3 to 80 at room temperature. The surface morphology of the catalyst was analyzed using the scanning electron microscope JEOL Model JSM-6390LV. UV-Visible diffuse reflectance data were collected over the spectral range 200-800 nm with a Varian Cary-500 UV–Vis–NIR spectrometer equipped with an integrating sphere attachment and Gamma alumina was used as the reference material. The photoluminescence emission spectra of the samples were measured at room temperature using Perkin-Elmer LS 55 Luminescence spectrophotometer.

2.4 Photocatalytic Studies

All the photocatalytic experiments were performed under natural sunlight on clear sky days during the period of February to April-2020. In a typical experiment, 50 ml of Reactive Orange 30 solution was taken with 50 mg of photocatalyst in a 250-ml glass beaker and saturated with oxygen by aerated with an air-pump and left aside for 1 hours to attain adsorption equilibrium. Then the dye solution was kept in direct sunlight with continuous aeration and the concentration of the dye remains was measured periodical by measuring its light absorbance at the visible λ_{max} by using a Elico UV-Visible spectrophotometer. In order to avoid the variation in results due to fluctuation in the intensity of the sunlight, a

set of experiments have been carried out simultaneously. the efficiency of the catalyst was calculated from the percentage of degradation of the dye solution. Combined oxidant photocatalytic degradation experiment also carried out above mentioned same method.

3. RESULT AND DISCUSSION

3.1 UV-Visible Analysis of Dye

The UV-Visible spectrum of the dye Reactive Orange 30 (RO 30) is as shown in the **Figure 3.1**. The dye shows maximum visible absorption at 430 nm and UV absorption at 235 nm. The visible absorbance at 430 nm has been used to calculate the concentration of dye solution before and after photocatalytic degradation experiments are by using Beer–Lambert law.

3.2 X-Ray Diffraction Studies

The XRD patterns of the TiO_2 and Sr, N-codoped TiO_2 samples synthesized in Sol-Gel method were given in **Figure 3.2**. The both TiO_2 and Sr, N -codoped TiO_2 shows diffraction peaks at 2θ values 25.4, 37.9, 48.1, 54.01, 55.02 and 62.80 arises from the diffraction from the planes (100), (004), (200), (105), (211), (116) and (215) respectively, which matches the standard JCPDS (21-1272) data of the anatase phase TiO_2 and there no peaks for other phases (rutile or brookite). The crystallite size of TiO_2 and Sr, N-codoped TiO_2 calculated using Debye−Scherrer equation formula was listed in **Table 3.1**. The results show that the Sr, N –codoping decreases the crystallite size of the TiO_2, the similar results were already reported for another non-metal doped TiO_2. The reason of decreasing crystal size of TiO_2 indicates, the codopant such as Sr, N is replacing Ti^{4+} sites.

3.3 Scanning Electron Microscopy(SEM) Analysis

SEM images of TiO_2, 0.001% Sr, N -codoped TiO_2, 0.003% Sr, N -codoped TiO_2, 0.005, Sr,N -codoped TiO_2, 0.007% Sr, N -codoped TiO_2 and 0.009% Sr, N -codoped TiO_2 calcinated at 450° C are shown in the **Figure 3.3**. SEM image of TiO_2 were irregular agglomerated spherical particle indicates in images that are coherent together of TiO_2 photocatalyst. But the 0.003% Sr, N -codoped TiO_2 and 0.005 Sr,N -codoped TiO_2 image there in highly separated smaller particles than pure TiO_2. This type of morphology might be efficiently adsorbed the dye molecules. Further increase the dopant (Sr, N) dosage to the TiO_2 lattice should be decrease good morphology manner, its due the aggregated surface of Sr, N -codoped TiO_2.

3.4 Diffused Reflectance UV-Visible Studies

The electronic bands of Sr, N -codoped TiO_2 samples were studied by using UV- diffused reflectance spectrum (**Figure 3.4**). A comparison of these curves indicates that the absorption edges of the Sr, N -codoped TiO_2 samples calcinated at 450°C are shifted to the longer wavelength region with respect to that of pure TiO_2. The conduction band and valence band of pure TiO_2 crystal consisted of the Ti_{3d} and O_{2p} states respectively. When TiO_2 was doped with B the N_{2p} and S_{3p} states were somewhat delocalized, so they greatly favored the formation of VB with O_{2p} and Ti_{3d} states. The formation of intrinsic band-gap TiO_2 slightly above the valence band due to the doping of B might be the reason for the red shift in the absorption of Sr, N -codoped TiO_2. The mixing of the 3p states of S with 2p state O may also increase the width of the VB.

3.5 Photocatalytic Studies

3.5.1 Photocatalytic Activity of Sr, N -codoped TiO_2

The photocatalytic activity of the photocatalysts was evaluated in the photodegradation of reactive orange (RO 30) at room temperature, under natural sunlight. RO 30 was slightly degraded under solar irradiation in the absence of catalyst. The evolution of the RO 30 concentration as a function of time is shown in **Fig 3.5**. Analyses of these curves were carried out with the Langmuir–Hinshelwood kinetic model:

After integration, we will get

$$-\ln\left(\frac{C}{C_0}\right) = k_{app}\, t$$

Where C_0 is the initial concentration (mg l^{-1}), C is the concentration of the dye after 't' minutes of illumination. The data obtained from the degradation of RO 30 fits well the apparent first order kinetics (**Figure 3.6**) and their rate constant values are given in the **Table 3. 2**. The dye degradation was found to be increases with the increase of Sr, N concentration in the studied level. Results suggest that doping of Sr, N was an effective way to improve the visible-light activity of TiO_2 based catalyst for the degradation of RO 30. The electrons in the conduction band can be transferred to surface adsorbed oxygen molecules and form superoxide anions, which can further transform to $OH^{\bullet}$ and initiate the degradation of RO 30. The fewer amount of surface hydroxyl groups were observed in case of Sr, N doped TiO_2 with higher dopants concentration. This could be reason for lower activity of Sr, N doped TiO_2 with higher Sr, N -doped concentration.

3.5.2 Photocatalytic Mechanism

The probable role of Sr, N in Sr, N codoped-TiO_2 photocatalyst was illustrated in

the **Figure. 3.6**. From the Figure, it could be seen that the Sr, N codoped-TiO_2 photocatalyst could be simultaneously excited to form electron–hole pairs. Due to this band position, the photoexcited electron on the CB of TiO_2 can be abstracted by oxidant (O_2). As a result, the electron and hole generated in the TiO_2 will have sufficient life time to prompt the photocatalytic oxidation reactions. However, the photogenerated electron in the CB of TiO_2 can react with oxidant such as oxygen molecule (O_2) to produce $^{\bullet}O_2^-$rather than undergoing recombination with holes in surface of TiO_2. Then, the $^{\bullet}O_2^-$ react with H^+ to give $HOO^{\bullet}$, which subsequently react with dye molecule in the solution. As a result, the photocatalytic activity of Sr, N codoped-TiO_2 photocatalyst was much higher than that of the wide band gap semiconductor TiO_2. Therefore, the enhancing photocatalytic activity of Sr, N codoped-TiO_2 was most possibly related to the codoped TiO_2 structure.

3.5.3 Reusability of Photocatalyst

To assess the stability of the catalyst on reuse, the same oxidant combined Sr, N codoped-TiO_2 was used in consecutive photocatalytic experiments for the degradation of RO 30 up to five cycles. The degradation of the 50 mg l-1 RO 30 dye solution at pH 3 over fresh oxidant combined Sr, N codoped-TiO_2 was 100% in two hours of sunlight irradiation. The used photocatalyst was separated after two hours of solar light irradiation and added to the fresh 50 mg l-1 dye solution on reuse the percentage of degradation observed was 100, 100, 98, 95 and 92 in the first, second, third, fourth and fifth reuse respectively (**Figure 3.8)**. The slight decrease in the activity of the photocatalyst after each cycle may be due to the residual intermediates of the degraded dye adsorbed on surface of photocatalyst. The results show that the reused oxidant combined Sr, N codoped-TiO_2 has about 96% of the activity of fresh catalyst in its third cycle. Hence it will be a good material for the degrading the organic dyes in textile effluents.

3.5.4 Effect of combined green oxidant Sr, N codoped TiO_2

Effect of H_2O_2 on the photodegradation efficiency Sr, N codoped TiO_2 for the degradation of RO 30 (100 mg/L) different concentrations of H_2O_2 was also carried out same experimental conditions were shown in **Fig. 3.9**.

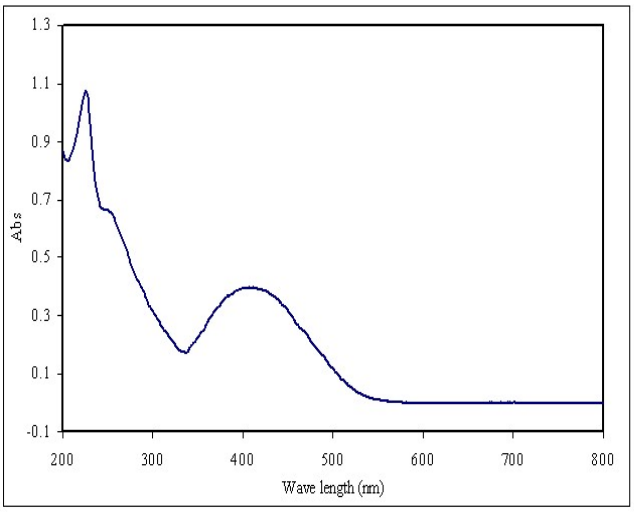

Figure 3. 1. UV-Visible absorbance spectrum of Reactive Orange 30

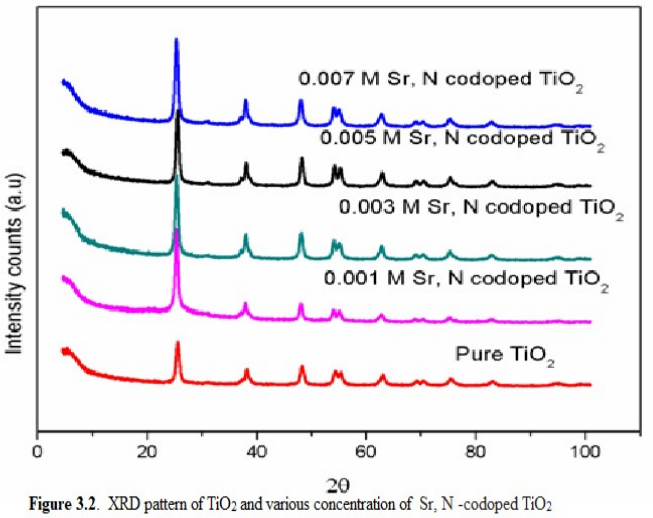

Figure 3.2. XRD pattern of TiO_2 and various concentration of Sr, N -codoped TiO_2

Photocatalyst	Crystallite size (nm)	d spacing (101) Å
TiO_2	17.06	3.52
0.005 % Sr, N -codoped TiO_2	15.78	3.50
0.007 % Sr, N -codoped TiO_2	12.73	3.53
0.009 % Sr, N -codoped TiO_2	12.38	3.50

Table 3.1. Crystallite size of photocatalyst calculated from XRD data

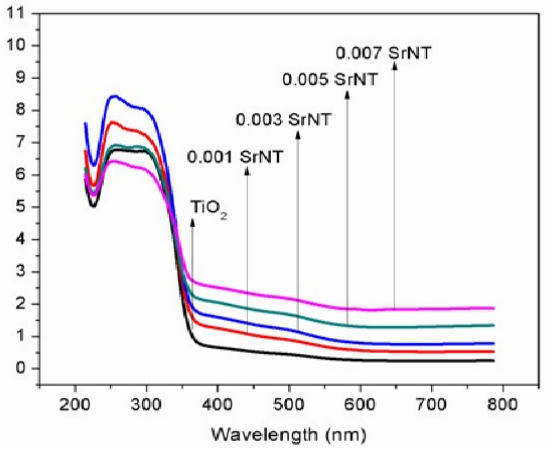

Figure 3.4 Diffused Reflectance Spectra of (a) TiO_2, (b) 0.001% Sr, N -codoped TiO_2 (c) 0.003% Sr, N -codoped TiO_2 (d) 0.005% Sr, N -codoped TiO_2 (e) 0.007% Sr, N -codoped TiO_2 (f) 0.009% Sr, N -codoped TiO_2

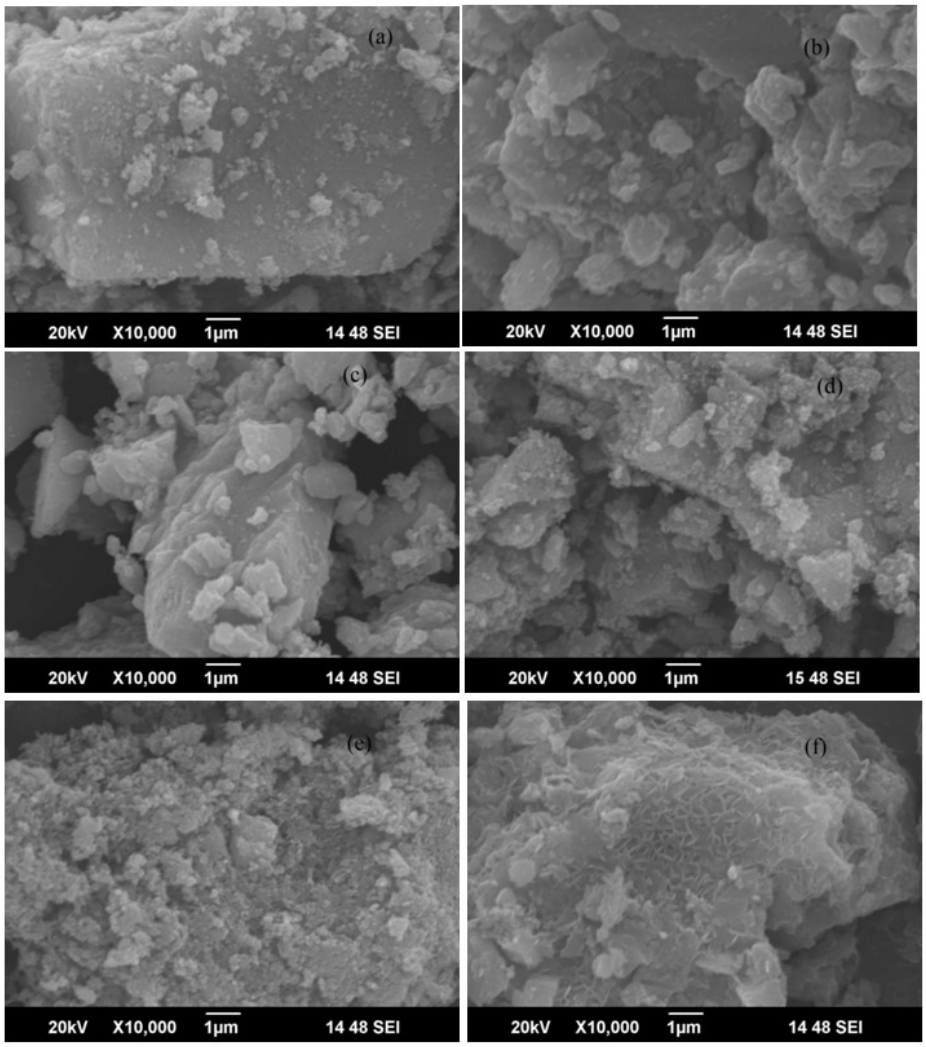

Figure 3.3: SEM image of the (a) TiO_2, (b) 0.001% Sr, N -codoped TiO_2 (c) 0.003% Sr, N -codoped TiO_2 (d) 0.005% Sr, N -codoped TiO_2 (e) 0.007% Sr, N -codoped TiO_2 (f) 0.009% Sr, N -codoped TiO_2

Table 3.2: Apparent first order rate constant values for the degradation RO 30 over Sr, N -codoped TiO_2

Photocatalyst	TiO_2	0.001% Sr, N-TiO_2	0.003% Sr, N-TiO_2	0.005% Sr, N-TiO_2	0.007% Sr, N-TiO_2	0.009% Sr, N-TiO_2
Apparent rate constant $K_{app}(min^{-1})$	0.0081	0.0122	0.0189	0.0230	0.0264	0.0168
R^2	0.9911	0.9947	0.9937	0.9909	0.9901	0.9905

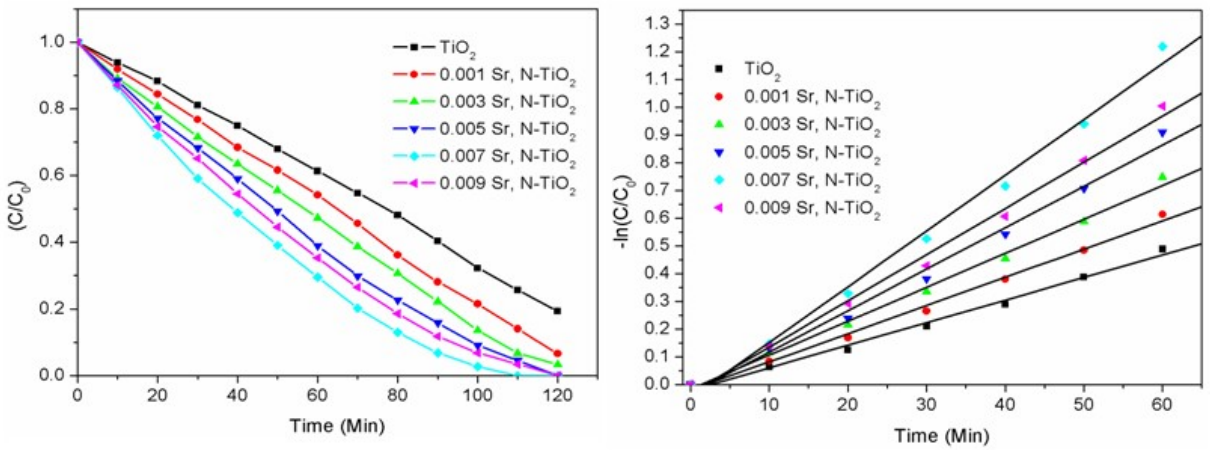

Figure 3.5: Photocatalytic degradation plots and Figure 3.6 Kinetics plots for the of degradation of RO 30 over Sr, N - codoped TiO_2

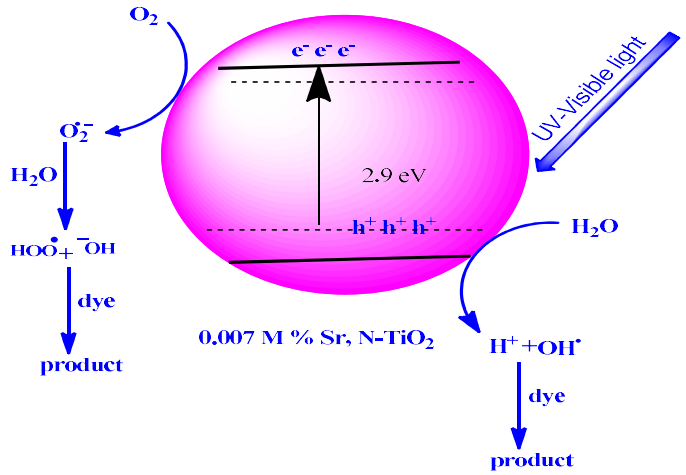

Figure 3.7: Proposed electron-hole charge separation mechanism

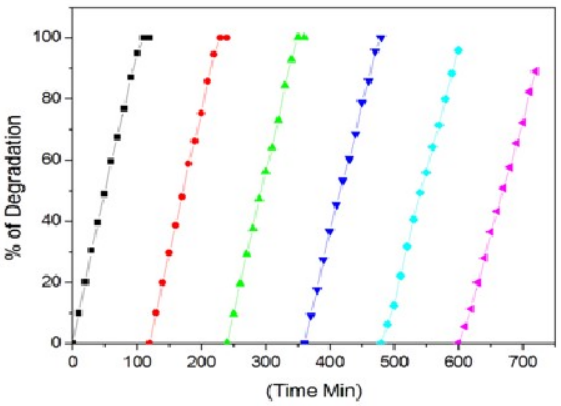

Figure 3.8 Reusability of oxidant combined Sr, N codoped-TiO_2

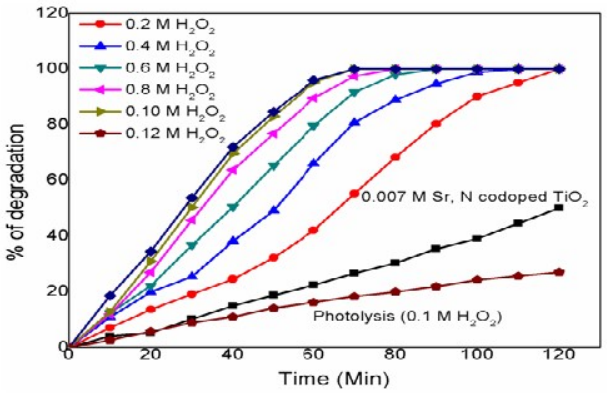

Figure 3. 9. Photocatalytic efficiency of Sr, N codoped TiO_2 photocatalyst at different H_2O_2 concentration for the degradation of RO 30.

The degradation efficiency of Sr, N codoped TiO_2 was increases with increasing amount of H_2O_2 0 mM (36%) to 12.5 mM (100%) under light irradiation. Further increasing H_2O_2 beyond 12.5 mM decreased the degradation efficiency. Hence, 12.5 mM of H_2O_2 is the optimal level for the degradation. The enhancement of degradation efficiency by the addition of H_2O_2 is due to the increased production of hydroxyl radicals and increasing the e^-_{CB}-/ h_{VB}^+ charge separation process as given in equations,

$$H_2O_2 + e^-_{CB} \longrightarrow {}^{\bullet}OH + {}^{-}OH \quad (1)$$

$$^{\bullet}OH + RB\,4 \longrightarrow \text{Degrade products} \quad (2)$$

Unexpectedly, the potential of photocatalytic efficiency decreases due to the presence of excess H_2O_2. This excess of H_2O_2 endagers the potential of photocatalytic activity by scavenging the highly valuable $^{\bullet}OH$ radical and produces much feeble $^{\bullet}OOH$.

$$H_2O_2 + {}^{\bullet}OH \longrightarrow {}^{\bullet}OOH + H_2O \quad (3)$$

$$^{\bullet}OOH + {}^{\bullet}OH \longrightarrow H_2O + O_2 \quad (4)$$

$$H_2O_2 + {}_{(VB)}h^+ \longrightarrow O_2 + H^+ \quad (5)$$

Further, the $^{\bullet}OOH$ reacts with remaining strong $^{\bullet}OH$ radical, leading to the formation of unfavorable H_2O and O_2 **[19]**. In addition, the photocatalytic oxidation found to be inhibited when the excess H_2O_2 reacted with oxidative h^+ on catalyst surface **(Eq. (5))**.The photodegradation capacity of H_2O_2 was also investigated in without photocatalysts (photolysis) on the degradation of RO 30 dye solutions under UV-visible light irradiation. Without Sr, N codoped TiO_2 photocatalyst, H_2O_2 alone causes 20% after 120 min irradiation.

CONCLUSION

Reactive azo dyes containing dichloro quinoxaline group have been successfully degraded over Sr, N codoped-TiO_2 photocatalyst in the presence sun light. Sr, N codoped-TiO_2 is enhances the photocatalytic activity in natural sunlight than the pure TiO_2. The rate of degradation of reactive orange 30 over Sr, N codoped-TiO_2 was higher in acidic pH when compared to neutral and basic conditions. The degradation

of RO 30 solution above 50 mg l-1 using Sr, N codoped-TiO_2 was more difficult due to degrade the dye solution. Sr, N codoped-TiO_2 has degraded 96 % of RO 30 in 2 h in its third reuse. The good activity of reused photocatalyst shows that these materials are cost-effective and can be reused many times. The use of H_2O_2 along with the Sr, N codoped-TiO_2increases the rate of degradation of RO 30 and also enables the degradation of dye solution with concentration above 100 mg/l. The optimum H_2O_2 concentration for the degradation of dyes on Sr, N codoped-TiO_2 was 0.10 M.

Acknowledgement

The authors acknowledge Sophisticated Test and Instrumentation Centre (STIC), Cochin University for the XRD and SEM facilities. One of the authors (MS) thanks the Periyar University, Salem, India, for providing fecilities for taking photoluminescence study for carrying out this research

REFERENCES

[1] B. O'Regan, Grätzel and M. A low-cost, high-efficiency solar cell based on dye-sensitized colloidal TiO_2 films. *Nature*, 353, 737− 740 1991.

[2] A. L. Linsebigler, G. Lu and J. T. Yates, Photocatalysis on TiO_2 surfaces: principles, mechanisms, and selected results. Chemical Review. 1995, 95, 735−758.

[3] Hadjiivanov, K. I.; Klissurski, D. G. Surface chemistry of titania (anatase) and titania-supported catalysts. *Chemical Society Review,* 25, 61−691996.

[4] M. Y. Xing, J. L. Zhang, F. Chen and B. Z. Tian, An economic method to prepare vacuum activated photocatalysts with high photoactivities and photosensitivities. *Chemical Communication* 47, 4947− 4949, 2011.

[5] S. Sato, Photocatalytic activity of NOx-doped TiO_2 in the visible light region. *Chemial and Physics Letter* 123, 126−128 1986.

[6] R. Asahi, T. Morikawa, T. Ohwaki, K. Aoki and Y. Taga, Visiblelight photocatalysis in nitrogen-doped titanium oxides. *Science* 2001, 293, 269−271.

[7] H. Irie, Y. Watanabe and K. Hashimoto, Nitrogen-concentration dependence on photocatalytic activity of TiO_2−xNx powders. *Journal of Physical Chemistry B* 107, 5483−5486 2003.

[8] J. H. Park, S. Kim, A. Bard, Novel carbon-doped TiO_2 nanotube arrays

with high aspect ratios for efficient solar water splitting. *Nanotechnology Lettrs* 6, 24−28 2006.

[9] Y. Cong, L. Xiao, J. L. Zhang, F. Chen and M. Anpo, Preparation and characterization of nitrogen-doped TiO_2 photocatalyst in different acid environments. *Research Chemical Intermediate* 32, 717−724 2006.

[10] W. K. Ho, J. C.Yu and S. Lee, Synthesis of hierarchical nanoporous F-doped TiO_2 spheres with visible light photocatalytic activity. *Chemical* Communication 10, 1115−1117 2006.

[11] Y. Cong, J. L. Zhang, F. Chen and M. Anpo, Synthesis and characterization of nitrogen-doped TiO_2 nanophotocatalyst with high visible light activity. *Journal of Physical Chemistry C*, 111, 6976−6982 2007.

[12] Li, H. X.; Zhang, X. Y.; Huo, Y. N.; Zhu, J. Supercritical preparation of a highly active S-doped TiO_2 photocatalyst for methylene blue mineralization. Environmental Science and Technology 2007, 41, 4410−4414.

[13] A. Emeline, V. Kuznetsov, V. Rybchuk and N. Serpone, Visiblelight-active titania photocatalysts: the case of N-doped TiO_2 sproperties and some fundamental issues. *International journal of Photoenergy*, 258394-1−19, 2008.

[14] M. Y. Xing, W. K. Li, Y. M.Wu, J. L. Zhang and X. Q. Gong, Formation of new structures and their synergistic effects in boron and nitrogen codoped TiO2 for enhancement of photocatalytic performance. *Journal of Physical Chemistry C*, 115, 7858−7865, 2011.

[15] A. P. Hong, D. W. Bahnemann and M. R. Hoffmann, Cobalt(II) tetrasulfophthalocyanine on titanium-dioxide-a new efficient electron relay for the photocatalytic formation and depletion of hydrogenperoxide in aqueous suspensions. *Journal of Physical Chemistry*, 91, 2109−2117 1987.

[16] Y. Mao, C. Schoneich, K. D. Asmus, Identification of organic acids and other intermediates in oxidative degradation of

chlorinated ethanes on titania surfaces en route to mineralization: a combined photocatalytic and radiation chemical study. *Journal of Physical Chemistry*, 95, 10080−10089 1991.

[17] K. Q. Huang, L. Chen, J. W. Xiong and M. X. Liao, Preparation and Characterization of Visible-Light-Activated Fe-N Co Doped TiO_2 and its Photocatalytic Inactivation Effect on Leukemia Tumors. International Journal of Photoenergy 2012 2012, 6314351−6314359.

[18] J. Q. Ding, Y. L. Yuan, J. S. Xu, J. Deng, and J. B. Guo, TiO2 Nanopowder Co-Doped with Iodine and Boron to Enhance VisibleLight Photocatalytic Activity. Journal of Biomedical Nanotechnology 5, 1-7, 2009.

[19] Saquib, M., M. Abu Tariq, M. Faisal and M. Muneer (2008) Photocatalytic degradation of two selected dye derivatives in aqueous suspensions of titanium dioxide. Desalination 219, 301–311.